

# On the decorrelation filtering of RL05 GRACE data for global applications

Santiago Belda Palazón, David García-García, and José Manuel Ferrándiz Leal

Department of Applied Mathematics, University of Alicante, Spain

Corresponding author: Santiago Belda Palazón, e-mail: [santiago.belda@ua.es](mailto:santiago.belda@ua.es)

This article has been published in **Geophysical Journal International** (2015, 200, 173–184) and undergone full peer review but has not been through the copyediting, typesetting, pagination and proofreading process which may lead to differences between this version and the Version of Record. Please cite this article as **doi:10.1093/gji/ggu386**. The definitive version is available at <http://gji.oxfordjournals.org/content/200/1/173.abstract?sid=a237d01f-56fe-4042-af16-de06ef2896d0>

## **Abstract**

In autumn 2012, the new release 05 (RL05) of monthly geopotential spherical harmonics Stokes coefficients (SC) from GRACE (Gravity Recovery and Climate Experiment) mission was published. This release reduces the noise in high degree and order SC, but they still need to be filtered. One of the most common filtering processing is the combination of decorrelation and Gaussian filters. Both of them are parameters dependent and must be tuned by the users. Previous studies have analyzed the parameters choice for the RL05 GRACE data for oceanic applications, and for RL04 data for global application. This study updates the latter for RL05 data extending the statistics analysis. The choice of the parameters of the decorrelation filter has been optimized to: (1) balance the noise reduction and the geophysical signal attenuation produced by the filtering process; (2) minimize the differences between GRACE and model-based data; (3) maximize the ratio of variability between continents and oceans. The Gaussian filter has been optimized following the latter criteria. Besides, an anisotropic filter, the fan filter, has been analyzed as an alternative to the Gauss filter, producing better statistics.

**Keywords:** Satellite geodesy; time-variable gravity; Spatial analysis.

## **1. Introduction**

The Gravity Recovery And Climate Experiment (GRACE) mission was launched in March 17, 2002. The GRACE mission measures the distance between two twin satellites in near polar orbit. These distances are used to estimate monthly geopotential spherical harmonics Stokes coefficients (SC), called Level 02 GRACE data, by Center for Space Research (CSR), GeoForschungsZentrum (GFZ), and Jet Propulsion Laboratory (JPL). Actually, these SC represent the geopotential differences with respect to a geopotential background, where some known geophysical processes are modeled: solid Earth and oceanic tides (including pole tides), non-tidal variability of the atmosphere and ocean, and gravity perturbations due

to the Sun, Moon and the rest of the planets (Bettadpur 2012; Dahle et al. 2013; Watkins & Yuan 2012).

Assuming that the geopotential variations are produced by mass changes at the surface of the Earth, it is possible to estimate the associated mass maps in form of millimeters of water thickness equivalent (WTE; Wahr et al., 1998; Chao, 2005). These maps show north-south stripes due to some noise in the high degree and order SC. So, they must be filtered to reduce that noise. However, there is not a standard filtering procedure and the GRACE users must decide which is the most convenient in their studies. There are several ways of filtering the data that can be found in the literature (Duan et al. 2009, and references therein). However, one of the most popular filtering procedures, due to its easy implementation, is a 2-step filter that firstly applies the decorrelation error filter (Swenson & Wahr 2006), and then the isotropic Gauss filter (Jekeli 1981; Swenson & Wahr 2002). The decorrelation filter has to be tuned for some parameters, which are left to the user's choice. Several authors have used different parameters depending on the application of the GRACE data (Chambers 2006; Chambers & Bonin 2012; Chen et al. 2007; Duan et al. 2009). In spite of the popularity of the Gaussian filter, the filtering process can be improved replacing it by an anisotropic filter that fits better the noise of the data (e.g., Chen et al., 2006; Zhang et al, 2009; García-García et al., 2010).

From time to time, the procedure to estimate the SC is improved and new sets of SC are released by the different agencies. In autumn 2012, a new release of GRACE data was published, called Release 05 (RL05). This new release presents less noise than previous releases due to the improvement in the knowledge of alignments between the star camera, accelerometer, and K-band ranging system for Level-1B data, and updated mean gravity field, ocean tide, pole tide, and de-aliasing models for Level-2 processing. Therefore, the parameters of the decorrelation filter must be tuned again. Chambers & Bonin (2012) optimized those parameters for ocean applications of the RL05 of GRACE data. In this study the choice of optimal parameters is explored for global applications of the same dataset, extending the work that Duan et al. (2009) did for the RL04 GRACE data. The 2-step filter

is also analyzed. The optimal radius of the Gauss filter is studied, as well as the application of an alternative anisotropic filter (Zhang et al, 2009).

## 2. Data Description and Methodology

The level 02 RL05 GRACE data from CSR, GFZ, and JPL are used in this study [<http://podaac.jpl.nasa.gov/gravity/grace>]. Data consists of monthly sets of SC spanning from 2004/01 to 2011/12 (except GFZ that starts in 2004/02), with missing values in 2011/01, and 2011/06. During the last months, some components of the GRACE satellites were disconnected in order to minimize the battery problems, and to extend the life of the mission as much as possible. The  $C_{20}$  coefficient is usually replaced by an estimate from Satellite Laser Ranging (Cheng & Ries 2007); it is excluded from the analysis. As far as we are interested in the variability of the geopotential, the mean value of the whole period is subtracted.

Assuming that the gravity variations are produced by mass variations on the surface of the Earth (such as the water mass transport within the water cycle, the biggest mass variations of the Earth in the intra-annual timescale), the surface mass variation,  $\sigma$ , in terms of WTE can be uniquely determined as:

$$\sigma(\theta, \lambda, t) = \frac{a\rho_E}{3} \sum_{l=0}^{\infty} \sum_{m=0}^l \frac{(2l+1)}{(1+k_l')} P_{lm}(\cos\theta) [C_{lm}(t)\cos(m\lambda) + S_{lm}(t)\sin(m\lambda)] \quad (1)$$

[Wahr et al., 1998; Chao, 2005], where  $(\theta, \lambda, t) = (\text{colatitude}, \text{longitude}, \text{time})$ ,  $a$  and  $\rho_E$  are the equatorial radius and the mean density of the Earth,  $k_l'$  is the degree- $l$  load Love number,  $P_{lm}$  is the  $4\pi$ -normalized associated Legendre function of degree  $l$  and order  $m$ , and  $C_{lm}(t)$  and  $S_{lm}(t)$  are the monthly GRACE SC.

Swenson & Wahr (2006) found, for a fixed order, a correlated error for the SC of even and odd degrees. They proposed a decorrelation filter that, for any SC of even (odd) degree, removes a polynomial fitted to some of the adjacent SC of even (odd) degree, which define a moving window. However, the degree of the polynomial or the length of the window was not specified and must be selected by the users. Besides, a portion of low degree and order SC is usually unfiltered, which must also be chosen by the users. An analysis of several configurations of the filter can be found in Duan et al. (2009), as those made (but not published) by Swenson & Wahr (2006), by Chambers (2006) for ocean applications, and by Chen et al. (2007) to study the 2004 Sumatra earthquake.

Duan et al. (2009) presented a configuration of the filter similar to Swenson & Wahr (2006). The idea is filtering stronger where the noise is higher, which can be achieved by increasing the order of the fitting polynomial or reducing the length of the window as the noise increase. They fixed the polynomial degree to 2 and vary the length of the window,  $\omega$ , accordingly to,

$$\omega = \max \left\{ A e^{-\frac{[(1-\gamma)m^p + \gamma l^p]^{\frac{1}{p}}}{k}} + 1, 5 \right\} \quad (2)$$

where  $l$  and  $m$  are the degree and order, respectively, of the SC to be filtered, which is located in the center of that window; and  $A$ ,  $k$ ,  $\gamma$ , and  $p$  are the parameters to be fixed, which define the filter itself. Figure 1 shows, for each degree and order, the length of the associated window accordingly to Equation 2 for a selection of parameters. They are clustered in bands, where number, width, slope, and curvature are defined by  $A$ ,  $k$ ,  $\gamma$ , and  $p$ , respectively. The width of the window decreases (increases) as  $A$  or  $k$  decreases (increases), which would make the filter stronger (weaker).

The minimum length of the window is fixed to 5 to retain some information after subtracting the polynomial of degree 2. In order to keep the SC to be filtered in the center of the window, the length of the latter is rounded to the nearest odd number. So, the polynomial of degree 2 to be subtracted from the SC of degree  $l$  and order  $m$ ,  $C_{lm}$  and  $S_{lm}$ , will be fitted to,

$C_{l-2\alpha,m}, \dots, C_{l-2,m}, C_{l,m}, C_{l+2,m}, \dots, C_{l+2\alpha,m}$ , and  $S_{l-2\alpha,m}, \dots, S_{l-2,m}, S_{l,m}, S_{l+2,m}, \dots, S_{l+2\alpha,m}$ , respectively, where  $\omega = 2 \cdot \alpha + 1$ . Only in the case that  $l$  is close to the maximum degree available in the data, or to the order  $m$ , the window is not centered in  $C_{lm}$  and  $S_{lm}$ .

Note that the decorrelation filter has been applied in a different way by Chambers (2006), Chambers & Bonin (2012), and Chen et al. (2007), who, for a fixed order, fitted and subtracted a single polynomial for all the SC of even or odd degree.

The low degree and order SC are less noisy, and for that reason are not usually filtered by the decorrelation filter. Based in a trial and error procedure, Chambers (2006) left unfiltered the SC with degree and order lower than 7 for RL02 GRACE data, and lower than 11 for RL04 GRACE data [[http://grace.jpl.nasa.gov/files/GRACE-dpc200711\\_RL04.pdf](http://grace.jpl.nasa.gov/files/GRACE-dpc200711_RL04.pdf)]. Chen et al. (2007) left unfiltered the SC of degree and order below 5 for RL04 GRACE data. On the other hand, Duan et al. (2009) chose the unfiltered SC based in the calibrated Standard Deviation (SD) provided by the agencies of the RL04 GRACE of one single month (as all the months look similar). They fit a curve to a SD value close to 1 ( $\times 10^{12}$ ) and left unfiltered the SC below that curve. For RL05 GRACE it is expected that the SD decrease with respect to former releases, and then the unfiltered portion of SC should be increased. For example, Chambers & Bonin (2012) showed that leaving unfiltered the SC with degree and order lower than 15 improves the statistics when comparing GRACE with ocean models. We will explore the influence of the unfiltered SC including an extra parameter,  $l$ , in the filter. Then, for each degree  $l$  we define a curve going from (degree, order)=( $l,0$ ) to (degree, order)=( $m,m$ ) that fits the SD in Figure 2. For example, for  $l=38$  the value of  $m$  is 11. Then, we left unfiltered the SC below that curve. In RL05, the calibrated SD are only available for GFZ GRACE data. We use the time average for the whole period of the formal (not calibrated) SD of the SC from GFZ and JPL data (they are not available for CSR data). Figure 2 shows the SD of the JPL GRACE data, which is similar to those from GFZ, and it is expected to be similar to those from CSR, as far as it was in previous releases.

The width of the moving window must vary accordingly to the noise of the data. So, the color bands shown in Figure 1 should be aligned with those in Figure 2. Following that

criteria it is easy to fix the parameters  $\gamma=0.04$ , and  $p=3.4$ . Then, the filter will be defined once the values of  $A$ ,  $k$ , and  $l$  are determined. We implement several experiments for a wide rank of parameters in order to define an optimal filter for global applications. In particular, GRACE and synthetic GRACE data (see below) are filtered with parameters:  $A$  from 10 to 24;  $k$  from 20 to 44; and  $l$  from 10 to 45. In order to reduce the high computational cost of the experiments, the parameters  $A$  and  $k$  vary 2 by 2, and  $l$  does 5 by 5 from 10 to 30, and 1 by 1 from 30 to 45.

For the following experiments we will need synthetic GRACE data, which consist of global grids with Ocean Bottom Pressure (OBP) over the oceans and with terrestrial water storage fields over land. The former is estimated from the ECCO (Estimating the Circulation and Climate of the Ocean; (Stammer et al. 2002); <http://www.ecco-group.org/products.htm>) model version kf080, and the latter is estimated from surface water storage grids from GLDAS/Noah (Global Land Data Assimilation Systems) model (Rodell et al. 2004; <http://disc.sci.gsfc.nasa.gov/hydrology/data-holdings>). These grids are estimated from the integration of 4-layer soil moisture, snow equivalent height and canopy water. As the hydrologic model has no data over Greenland and Antarctica, these regions are avoided in the comparison with GRACE. In order to make the synthetic data more realistic an estimate of the Post Glacial Rebound (PGR) from Paulson et al. (2007) have been added to the grids. The synthetic data have been reduced to  $1^\circ \times 1^\circ$  monthly grids for the period 01/2004–12/2011, and transformed to mm of WTE ( $\text{kg/m}^2$ ). The mean value of the whole period is removed from the signal. The points covered neither by GLDAS/Noah nor ECCO are set to zero. When the filter is applied to the synthetic data, the degree-1 and the  $C_{20}$  coefficients are set to zero.

### **3. First-step filter**

#### **3.1 Linear trends**

When filtering the data, the noise is reduced jointly with some of the sought geophysical signals. On the one hand, if the filter is very weak the noise will dominate the signal. On the other hand, if the filter is very strong the geophysical signal will be too attenuated. In some place between these two opposite cases resides the optimal filtering level. In order to find the latter, we explore the strategy used by Duan et al. (2009) to select the parameters of the filter for RL04 GRACE data, who found the values  $A=30$ ,  $k=15$ ,  $\gamma=0.1$ ,  $p=2$  for CSR data, and  $A=30$ ,  $k=15$ ,  $\gamma=0.1$ ,  $p=3$  for JPL data. The selection is based on the study of the root mean square (RMS) of the lineal trend of surface mass grids from GRACE and synthetic data. The unfiltered GRACE data present too high linear trend values, with an associated high RMS, due to noise influence. So, the reduction of such trends (and associated RMS) would indicate a reduction of the noise. However, an excessive reduction would mean an undesirable attenuation of the geophysical signals. In order to estimate the latter, the filter is applied to noise-free data based on models, the synthetic data. The perfect filter should not reduce the trends of noise-free data. The optimal filter should minimize the RMS of the global linear trend in GRACE data, and maximize them in synthetic data. In practice, the RMS of the filtered GRACE and synthetic data are normalized with respect to their RMS prior to filtering. This is made to reduce the influence of the high values produced by very noisy GRACE data. After normalization, the linear trend RMS from synthetic data present higher values than those from GRACE data. It makes sense since the filter produces attenuation of the signal in both data, but noise reduction only in GRACE data. Therefore, the optimal filter should maximize the difference between the linear trends RMS of synthetic and GRACE data. Figure 3 shows the latitude weighted RMS of the linear trends for synthetic, and the three agencies GRACE data, and Figure 4 shows their differences. Each value is estimated using a different combination of  $A$ ,  $k$ , and  $l$ . The parameter  $l$  shows de greatest gradient, with optimal values between 35 and 45, and several combinations of  $A$  and  $k$ . For example, for CSR and  $l=38$ , the greatest differences can be reached around  $(A,k)=(24,20)$ . This experiment gives an idea about the importance of the parameter  $l$ , and justifies the finer resolution between 30 and 45. However, the choice of the parameters is too vague and further analyses are needed.

### **3.2 GRACE Vs Synthetic data**



GRACE and synthetic data are compared, but some preliminary corrections must be made to the GRACE data. Firstly, as synthetic data represent OBP over the ocean, GRACE should represent the same. It is reached in two steps: (1) the atmospheric and oceanic corrections applied to GRACE over the ocean, the GAD product, is added back, (2) for each month the global ocean Sea Level Pressure (SLP, from NCEP) average is subtracted from the ocean points in GRACE. Note that the GAD and SLP data are not filtered, so they may modify the absolute values of the linear trends experiment, but not the relative values among them, which we were interested in the previous experiment. Secondly, to make the spatial resolution comparable the synthetic grids are transformed into SC, and then back to grids only using SC up to degree 60. In the processes the degree-1 and  $C_{20}$  coefficients are suppressed. No filter is applied. Finally, the regions not covered by the synthetic data – Antarctica, Greenland and Arctic ocean- are discarded in the analysis, and the continental leakage is reduced (Wahr et al. 1998).

Since the decorrelation filtered GRACE data are still too noisy to be compared to the unfiltered synthetic data, a Gaussian filter of 500 km radius is also applied to the former. The Gaussian filter is defined by a radius  $r$ , and consists of the application of a weight,  $W_l^r$ , to the SC (see Swenson and Wahr, 2002, for a recursive formula). Then, the surface mass grids are estimated as

$$\sigma(\theta, \lambda, t) = \frac{a\rho_E}{3} \sum_{l=0}^{\infty} \sum_{m=0}^l \frac{(2l+1)}{(1+k_l)} W_l^r P_{lm}(\cos\theta) [C_{lm}^*(t)\cos(m\lambda) + S_{lm}^*(t)\sin(m\lambda)], \quad (3)$$

where  $C_{lm}^*(t)$  and  $S_{lm}^*(t)$  are the SC once the decorrelation filter has been applied. Note that the only other difference with Eq. 1 is the term  $W_l^r$ .

For each grid point the RMS of the difference between filtered GRACE and unfiltered synthetic data is estimated. Figure 5 shows the spatial average of these RMS for different parameters of the filter. The minimum values are reached with parameters  $36 \leq l \leq 39$ ,  $10 \leq A \leq 16$ , and  $20 \leq k \leq 28$ . Similarly, the correlation coefficient between filtered GRACE and unfiltered synthetic data is shown in Figure 6. The maximum correlations are reached with

$38 \leq l \leq 39$ ,  $A \sim 14$ , and  $20 \leq k \leq 28$  for CSR data, and with  $36 \leq l \leq 40$ ,  $10 \leq A \leq 14$ , and  $20 \leq k \leq 28$  for GFZ and JPL data. Therefore, for all GRACE datasets the minimum residual and the maximum correlation is reached around the same parameters, narrowing the parameters values selected by the linear trends experiment.

It is worthwhile to remark that the minimum difference between GRACE and synthetic do not necessary define the optimal filter. The reason is that GRACE measures signals that hydrological models generally do not account for, as for example groundwater, river storage or water extraction from aquifers. Besides, during the filtering process the signal amplitude is attenuated and it must be restored to approximate the real signal, which can be done for regional averaged signals (e.g., Velicogna & Wahr, 2006) or grid points (Landerer & Swenson, 2012). In the restoring amplitude process the differences with the synthetic data are not necessarily reduced. On the other hand, the correlation coefficient does not depends on whether the amplitude of a time series is restored, since the restoring factor is a constant multiplying the whole time series.

The annual amplitude has been estimated for each grid point of GRACE and synthetic data. Figure 7 shows the correlation coefficients between them. The maximum correlation is reached for the greatest values of  $A$ ,  $k$ , and  $l$ , that is, for the weakest version of the filter. It makes sense since the estimation of the annual amplitudes acts as a filter itself. On the other hand, Figure 8 shows that a stronger version of the filter with lower  $l$  is needed to reach the maximum correlation of the non-seasonal signals (no linear trend nor annual amplitude). It means that a modification of the parameters must be considered depending on the sought-after signal.

### **3.3 Continents Vs Ocean**

The optimal filter can also be explored using the criteria that Chen et al. (2007) defined for tuning their anisotropic filter. The idea is based on the fact that the surface mass variability is stronger in the continents than in the oceans. The ratio of variability can be measured as the

quotient of the latitude weighted RMS of the continental and oceanic signals. On the one hand, if some noise were added to the SC, spurious variability would be introduced in both continents and oceans. On the other hand, if the SC were attenuated the variability in both continents and oceans would be reduced. In any case, the ratio of variability between the continents and the ocean would be reduced. So, the maximum of such ratio would represent the maximum of signal-to-noise ratio, which should be obtained using the optimal filter. Figure 9 shows the values of that ratio for several decorrelation filters, as well as a Gaussian filter of 500 km, for data from the three agencies. In order to reduce the leakage of the continental signal only the ocean points farther than 500 km from the coast are included. The maximum ratios are obtained with  $38 \leq l \leq 43$ ,  $14 \leq A \leq 16$ , and any  $k$  for CSR data, and with  $38 \leq l \leq 41$ ,  $12 \leq A \leq 14$ , and any  $k$  for GFZ and JPL data.

### 3.4 Parameters selection

Accordingly to the previous experiments some conclusions can be made: (1) The three agencies show a similar noise distribution, but not identical; (2) The portion of unfiltered SC is the most critical parameter; (3) As the latter has increased from RL04 to RL05, it can be inferred that RL05 data are less noisy than RL04; (4) The optimal statistics of the experiments is not reached for a unique parameters configuration, but for all the agencies it can be reached with parameters values close to  $l=38$ ,  $A=14$ , and  $k=24$ .

In sections 3.2 and 3.3, a Gaussian filter with a radius of 500 km was also applied to GRACE data. In order to check whether that choice could vary the optimal parameters of the decorrelation filter, the same analysis was implemented with a radius of 300 km. In that case, the obtained results were quite similar.

## 4. Second-step filter

Once the decorrelation error filter is applied, a second filter must be applied, which generally is the isotropic Gaussian one. The parameter  $r$  defining the filter approximately fixes the spatial resolution of the filtered grids. Figure 10 shows the weights  $W_i^r$  of the Gaussian filter

for different radius. Note that the weight of high degree SC decreases as  $r$  increases, that is, the spatial resolution decreases as  $r$  increases. The parameter  $r$  is usually fixed with a visual trial and error procedure looking for grids without north-south stripes. However, an optimal  $r$  could be found objectively maximizing the ratio of variability between continents and oceans as in section 3.3 (Chen et al., 2007). Figure 11 shows the evolution of this ratio, which has been estimated only including the ocean points farther than 500 km from the coast to reduce the leakage from the continental signal. The maximum ratio, and then the optimal Gaussian filter, is obtained with  $r=380$  km for CSR,  $r=420$  km for GFZ, and  $r=400$  km for JPL. The maximum ratio in CSR and GFZ data is  $\sim 3.5$ , while it is 3.3 for JPL data.

Note that the radius  $r$  roughly represents the spatial resolution of the WTE maps. However, the resolution is limited to  $20000/N$  km, where  $N$  represents the truncation degree of the SC. So, if  $N=40$  and  $N=60$  a maximum spatial resolution of 500 km and  $\sim 333$  km could be reached, respectively. For that reason, the reported values of  $r$  must be interpreted carefully.

In order to estimate the error of the data, the residuals of the differences between GRACE and synthetic data are explored as in section 3.2, but using the optimal  $r$  of each agency. Then, the standard deviation of the residual is estimated for each grid point. Figure 12 shows the residual for the CSR, GFZ, and JPL data using SC up to degree 60, which are very similar. The global latitude-weighted averaged of the residuals are 26.1 mm for CSR and GFZ, and 26.5 mm for JPL. The largest signal is observed around Greenland, which is not modeled by the hydrological model, and in the Amazon, where the surface waters are neither modeled. When these two regions are avoided the residuals are reduced to 24.6 mm for CSR and GFZ and 25.0 mm for JPL. Besides, when the continental leakage is reduced, the residual drops around 1.5%. In any case, remember that noise-free GRACE data are not expected to minimize the residual.

The 2-step filtering process can be improved replacing the isotropic (only degree dependent) Gauss filter by an anisotropic (degree and order dependent) filter. The Gaussian filter applies weights to the SC that decreases as the degree increases. The fan filter is a combination of two Gaussian filters, one applied to the degrees, and another to the orders (Zhang et al,

2009). Then, the fan filter can be defined with two radii, one for the degrees,  $r_l$ , and another for the orders,  $r_m$ . In this case, the surface mass grids are estimated as

$$\sigma(\theta, \lambda, t) = \frac{a\rho_E}{3} \sum_{l=0}^{\infty} \sum_{m=0}^l \frac{(2l+1)}{(1+k_l')} W_l^{r_l} W_m^{r_m} P_{lm}(\cos\theta) [C_{lm}^*(t)\cos(m\lambda) + S_{lm}^*(t)\sin(m\lambda)], \quad (4)$$

where the weights  $W_l^{r_l}$  and  $W_m^{r_m}$  depends on the degree  $l$  and order  $m$ , respectively. Note that the only difference with Eq. 3 is the term  $W_m^{r_m}$ .

In the Gauss filter the radio  $r$  roughly represents the spatial resolution in any direction, while  $r_l$  and  $\sqrt{2} \cdot r_m$  represent the north-south and east-west spatial resolution, respectively. Similarly to the Gauss filter, the optimal radii of the fan filter are explored to maximize the ratios of variability between continents and oceans. Figure 13 shows that the largest ratios are reached with radii close to  $(r_l, r_m) = (290, 690)$  km for CSR,  $(r_l, r_m) = (310, 820)$  km for GFZ, and  $(r_l, r_m) = (290, 640)$  km for JPL. The obtained ratios are larger with the fan filter than with the Gauss filter. Although, the residuals of the differences between GRACE and synthetic data look similar (not shown), their average is 25.4 mm for CSR, 25.3 mm for GFZ, and 26.1 mm for JPL. When the points from Amazon and around Greenland are excluded, the residuals are reduced to 23.9 mm for CSR and GFZ, and 24.6 mm for JPL. In any case, the residuals are smaller than using the Gauss filter. Then, the fan filter seems to be more appropriated than the Gauss filter as second-step filter.

#### 4. Discussion

GRACE data must be filtered before use to reduce some noise in high degree and order SC. One of the most popular filters is a 2-step filter: (1) decorrelation filter and (2) Gauss filter. Both filters must be adapted to the noise level of the data. While the Gauss filter only depends on one parameter, the decorrelation filter depends on several parameters producing multiple combinations. In this study we have analyzed the parameters configurations of the decorrelation filter for the RL05 of GRACE data that optimize several statistics for global applications. These parameters are close to  $l=38$ ,  $A=14$ , and  $k=24$ , as well as  $\gamma=0.04$  and

$p=3.4$ , for all the agencies. Besides, the application of the isotropic Gauss filter and the anisotropic fan filter as second-step filter has been analyzed. The best results for the Gauss filter are obtained with  $r=380$  km for CSR,  $r=420$  km for GFZ, and  $r=400$  km for JPL, while for the fan filter are obtained with values close to  $(r_l, r_m)=(290,690)$  km for CSR,  $(r_l, r_m)=(310,820)$  km for GFZ, and  $(r_l, r_m)=(290,640)$  km for JPL.

Table 1 summarizes the analyzed statistics of the reported filters, as well as those using parameter configuration from previous studies. In order to make the different filters comparable, the calculation are made using SC up to degree 40 as in Chambers & Bonin (2012), and up to degree 60 as in Duan et al. (2009), and Chen et al. (2007). In both cases, and for any agency, the parameters estimated in this study show: (1) smaller RMS values in the linear trends of GRACE data; (2) smaller differences and larger correlation with the synthetic data; (3) larger variability ratios between continents and ocean signals, which are reached with (4) smaller radius in the Gaussian filter. From these results it can be inferred that the filtering parameters estimated in this study present a more optimal compromise between noise elimination and geophysical signals preservation, and a better spatial resolution. The result is not surprising since Duan et al. (2009) proposed a filter for the RL04 data, and Chambers & Bonin (2012) for ocean applications. When regarding to the ocean the latter filter produces a RMS of the differences  $\sim 16$  mm for the three agencies, which is similar to the value obtained using the reported parameters and Gauss filter. The global statistics using the fan filter are summarized in Table 2, and they improve those from the Gaussian filter. As the Gauss and the fan filter are both easily implemented, the latter should be consider as second-step filter.

The selection of the parameters, and hence the design of the 2-step filter depends on the models used in the synthetic data. However, the study of the variability between continents and oceans does not depend on the model and gives an approximation of the filter. Then, the results are not expected to vary significantly as the models change.

This study complements the one done by Chambers & Bonin (2012) for oceanic applications, and it could be of interest for GRACE users that would like to continue processing the RL05 data with the decorrelation filter.

### **Acknowledgement**

We thank all the organizations providing the used data: time-variable gravity data provided by the GRACE team; GLDAS hydrological data by GSFC/NASA; ocean bottom pressure by ECCO Group; SLP from NCEP. This work has been partly supported by two Spanish Projects from CGL2010-12153-E and AYA2010-22039-C02-01; and two from Generalitat Valenciana, GV/2013/144 and ACOMP-2013-068.

### **References**

- Bettadpur, B., 2012. CSR Level-2 processing standards document for product release 05 GRACE 327–742, revision 4.0. Available at <http://podaac.jpl.nasa.gov/gravity/grace-documentation>
- Chambers, D. P., 2006. Evaluation of new GRACE time-variable gravity data over the ocean, *Geophys. Res. Lett.*, 33:L17603, doi:10.1029/2006GL027296.
- Chambers, D. P. & Bonin, J. A., 2012. Evaluation of Release-05 GRACE time-variable gravity coefficients over the Ocean, *Ocean Sci. Discuss.*, 9, 2187-2214, doi:10.5194/osd-9-2187-2012.
- Chao, B. F., 2005. On inversion for mass distribution from global (time-variable) gravity field, *J. Geodyn.*, 39, 223–230, doi:10.1016/j.jog.2004.11.001.

- Chen, J. L., Wilson, C. R., and Seo, K.-W., 2006. Optimized smoothing of Gravity Recovery and Climate Experiment (GRACE) time-variable gravity observations, *J. Geophys. Res.*, 111, B06408, doi:10.1029/2005JB004064.
- Chen, J. L., Wilson, C. R., Tapley, B. D. & Grand, S., 2007. GRACE detects coseismic and postseismic deformation from the Sumatra-Andaman earthquake, *Geophys. Res. Lett.*, 34, L13302, doi:10.1029/2007GL030356.
- Cheng, M. & Ries, J., 2007. GRACE technical note 05: Monthly estimates of C20 from 5 SLR satellites. Available at <http://podaac.jpl.nasa.gov/grace/documentation.html>.
- Dahle, C., Flechtner, F., Gruber, C., König, D., König, R., Michalak, G. & Neumayer, K.-H., 2013. GFZ GRACE Level-2 Processing Standards Document for Level-2 Product Release 0005, revision 1.1. Available at <http://podaac.jpl.nasa.gov/gravity/grace-documentation>
- Duan, X. J., Guo, J. Y., Shum, C. K. & Van der Wal, W., 2009. On the postprocessing removal of correlated errors in GRACE temporal gravity field solutions, *J. of Geod.*, 83, 1095–1106, doi:10.1007/s00190-009-0327-0.
- García-García, D., Chao, B. F., and Boy, J.-P., 2010. Steric and mass-induced sea level variations in the Mediterranean Sea revisited, *J. Geophys. Res.*, 115, C12016, doi:10.1029/2009JC005928.
- Jekeli, C., 1981. Alternative methods to smooth the Earth's gravity field, *Dep. of Geod. Sci. and Surv., Ohio State Univ (Columbus)*.
- Landerer, F. W., & Swenson, S. C., 2012. Accuracy of scaled GRACE terrestrial water storage estimates, *Water Resour. Res.*, 48, W04531, doi:10.1029/2011WR011453.



- Paulson, A., Zhong, S. & Wahr, J., 2007. Inference of mantle viscosity from GRACE and relative sea level data, *Geophys. J. Int.*, 171, 497-508, doi: 10.1111/j.1365-246X.2007.03556.x
- Rodell, M., Houser, P. R., Jambor, U., Gottschalck, J., Mitchell, K., Meng, C.-J. et al., 2004. The global land data assimilation system, *Bulletin of the American Meteorological Society*, 85(3), 381–394, doi:10.1029/2004GL020873.
- Swenson, S., & Wahr, J., 2002. Methods for inferring regional surface mass anomalies from Gravity Recovery and Climate Experiment (GRACE) measurements of time-variable gravity, *J. Geophys. Res.*, 107(B9), 2193, doi:10.1029/2001JB000576.
- Swenson, S., & Wahr, J., 2006. Post-processing removal of correlated errors in GRACE data, *J. Geophys. Res.*, 33, L08402, doi:10.1029/2005GL025285.
- Velicogna, I. & Wahr, J., 2006. Measurements of Time-Variable Gravity show Mass Loss in Antarctica, *Science* 311, 1754-1756.
- Wahr, J., Molenaar, M. & Bryan, F., 1998. Time-variability of the Earth's gravity field: Hydrological and oceanic effects and their possible detection using GRACE, *J. Geophys. Res.*, 103, 30205– 30229.
- Watkins, M. M. & Yuan, D.-N., 2012. JPL Level-2 Processing Standards Document for Level-2 Product Release 05, revision 5.0. Available at <http://podaac.jpl.nasa.gov/gravity/grace-documentation>
- Zhang, Z., Chao, B. F., Lu, Y., & Hsu, H., 2009. An effective filtering for GRACE time-variable gravity: Fan filter, *Geophys. Res. Lett.*, 36, L17311, doi:10.1029/2009GL039459.

		Decorrelation		Decorrelation and Gauss filters			
			RMS linear trend (mm/year)	RMS differences (mm)	Correlation Coefficients	Ratio Cont/ocn	r (km)
Degree 60	<i>Chen et al. (2007)</i>	CSR	10.7	25.8	0.53	3.27	500
		GFZ	10.8	25.6	0.52	3.27	600
		JPL	11.0	26.3	0.52	2.98	540
	<i>Duan et al. (2009)</i>	CSR	10.8	25.8	0.53	3.32	490
		GFZ	-	-	-	-	-
		JPL	11.5	25.9	0.53	3.03	540
	This study	CSR	9.7	26.1	0.54	3.53	380
		GFZ	9.6	26.1	0.52	3.52	420
		JPL	9.6	26.5	0.53	3.31	400
Degree 40	<i>Chambers &amp; Bonin (2012)</i>	CSR	9.2	26.3	0.52	3.35	430
		GFZ	9.0	25.8	0.52	3.37	520
		JPL	9.0	26.6	0.52	3.09	480
	This study	CSR	8.9	26.1	0.53	3.54	380
		GFZ	8.7	26.1	0.52	3.52	420
		JPL	8.7	26.4	0.53	3.32	400

**Table 1.** For the three agencies of GRACE data: RMS of linear trends from decorrelation filtered GRACE data. RMS of the differences and correlation coefficients between GRACE (decorrelation and Gauss filters) and synthetic data. Maximum ratio of variability continents/oceans from decorrelation and Gauss filtered GRACE data, as well as the radio where the maximum is reached. For comparison purposes the maximum degree is set to 40 and 60.

		Decorrelation and fan filters			
		RMS differences (mm)	Correlation Coefficients	Ratio Cont/ocn	$r_l / r_m$ (km)
Degree 60	CSR	25.4	0.55	3.68	290 / 690
	GFZ	25.3	0.53	3.73	310 / 820
	JPL	26.1	0.54	3.45	290 / 640
Degree 40	CSR	25.3	0.54	3.70	290 / 690
	GFZ	25.3	0.53	3.75	310 / 820
	JPL	25.9	0.53	3.48	290 / 640

**Table 2.** As Table1, but fan filter is used instead of Gauss filter.

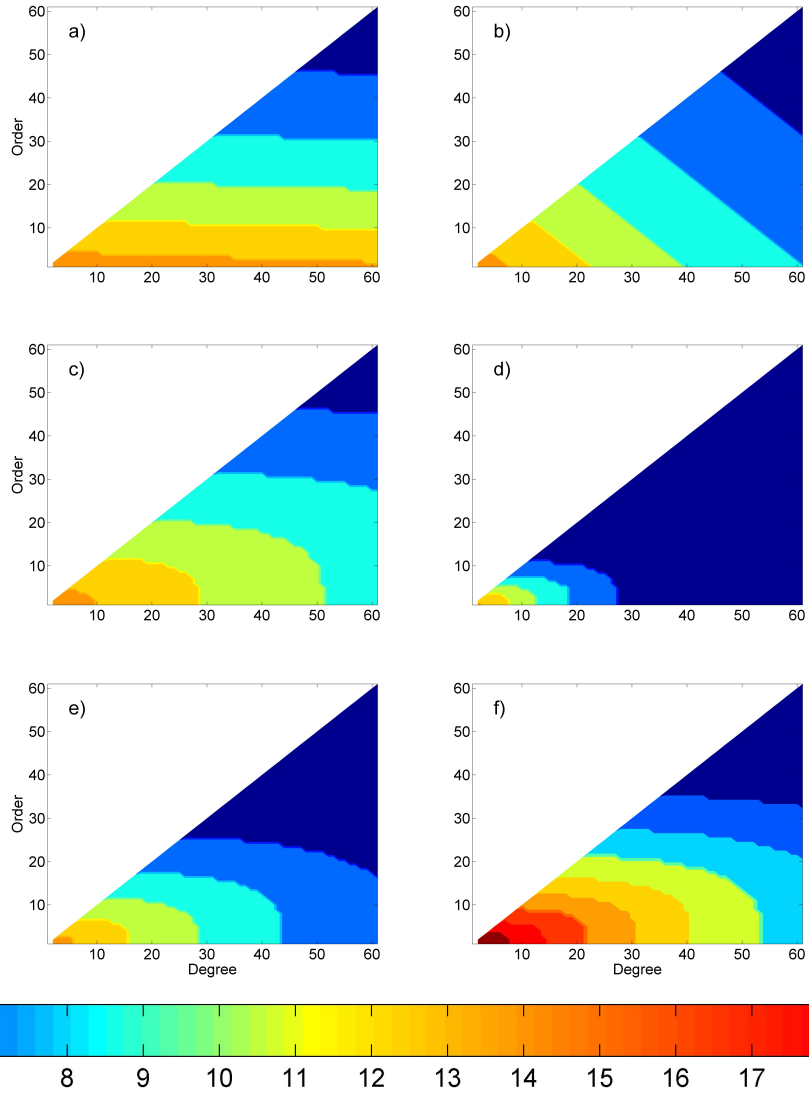


**Figure 1.** Length of the window accordingly to Equation 2 for each degree and order, and for different parameters configurations: a)  $A=14, k=44, \gamma=0.04, p=1$ ; b)  $A=14, k=44, \gamma=0.5, p=1$ ; c)  $A=14, k=44, \gamma=0.04, p=3.4$ ; d)  $A=14, k=10, \gamma=0.04, p=3.4$ ; e)  $A=14, k=24, \gamma=0.04, p=3.4$ ; f)  $A=21, k=24, \gamma=0.04, p=3.4$ .

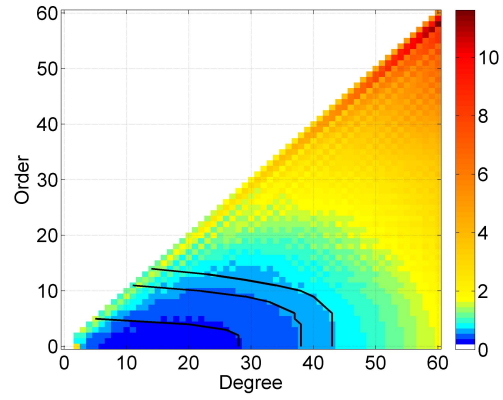


**Figure 2.** Time average of the formal (not calibrated) SD (scaled by  $\times 10^{12}$ ) of the JPL RL05 GRACE SC. Black lines represent the curves delimiting the unfiltered SC for  $l=28, 38$  and  $43$ .

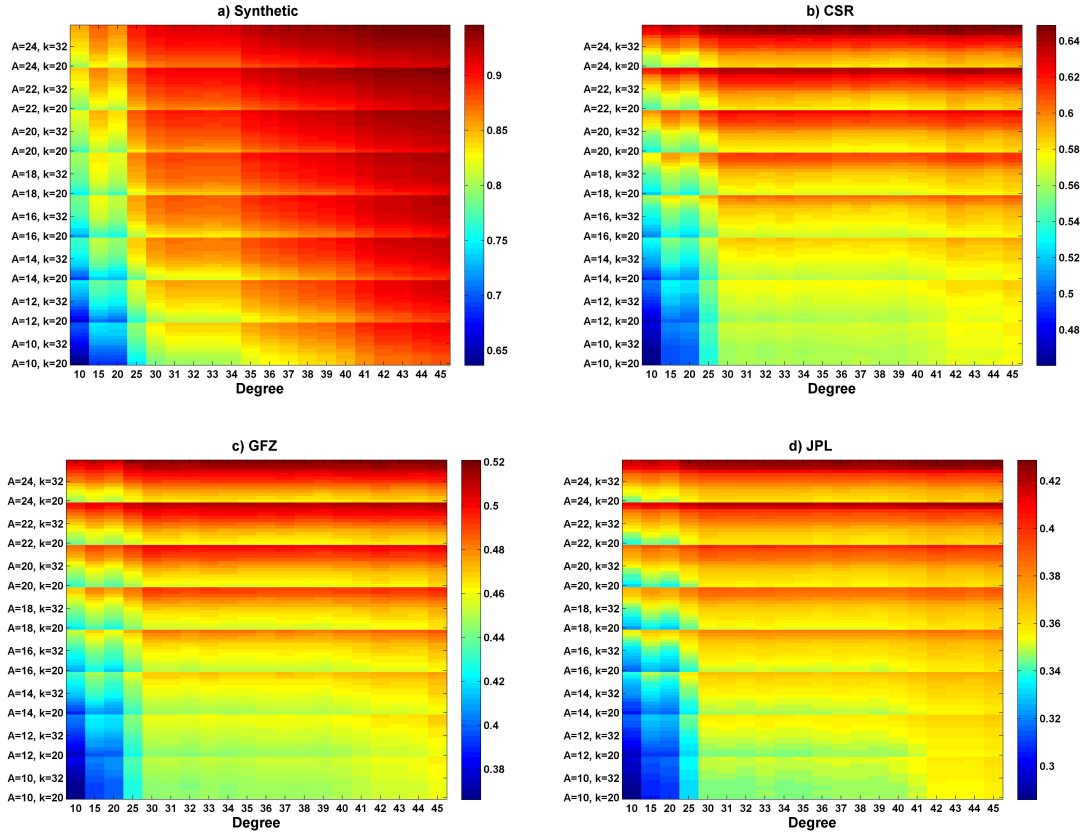


**Figure 3.** RMS of the linear trends from a) synthetic, and GRACE data: b) CSR; c) JPL; and d) GFZ. Each value is estimated using a decorrelation filter with different combination of  $A$  (from 10 to 24, 2 by 2),  $k$  (from 20 to 44, 2 by 2), and  $l$  (5 by 5 from 10 to 30, and 1 by 1 from 30 to 45). Units: Percentage with respect to RMS prior filtering.

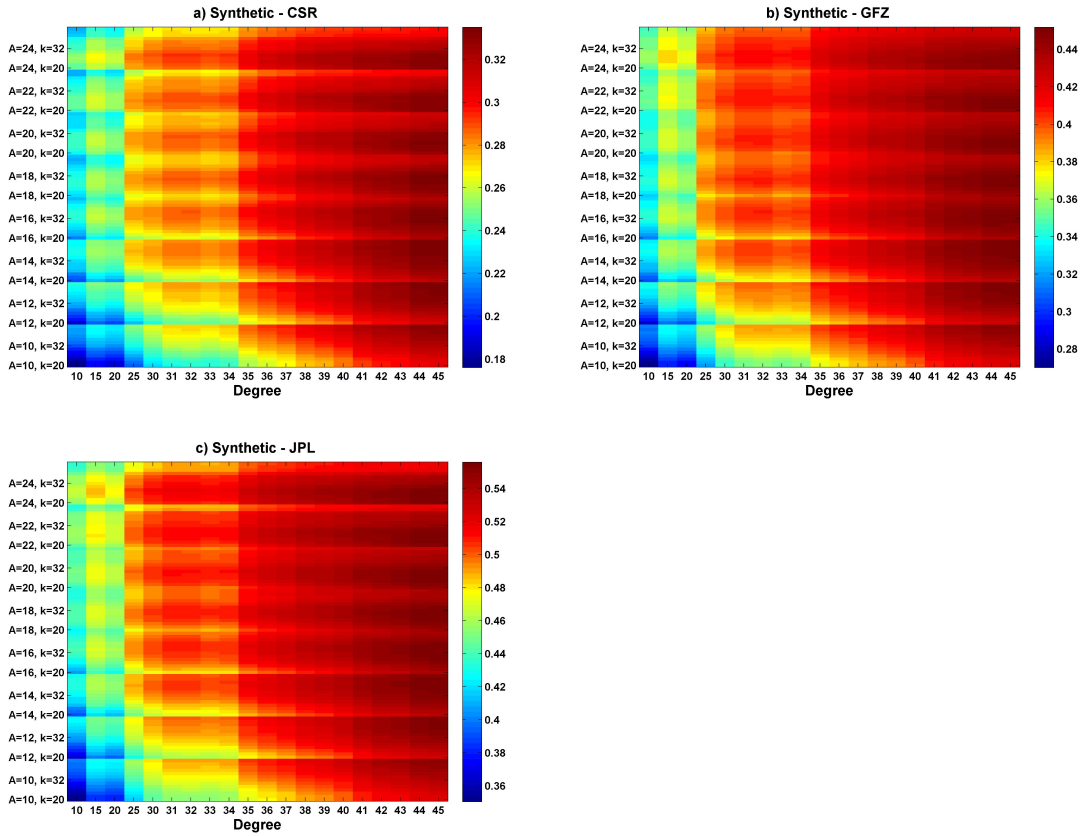


**Figure 4.** Differences between the RMS of the linear trends from synthetic and GRACE data: a) CSR; b) GFZ, and c) JPL. Decorrelation filter applied to GRACE and synthetic data prior subtraction. Units: Percentage with respect to RMS prior filtering.

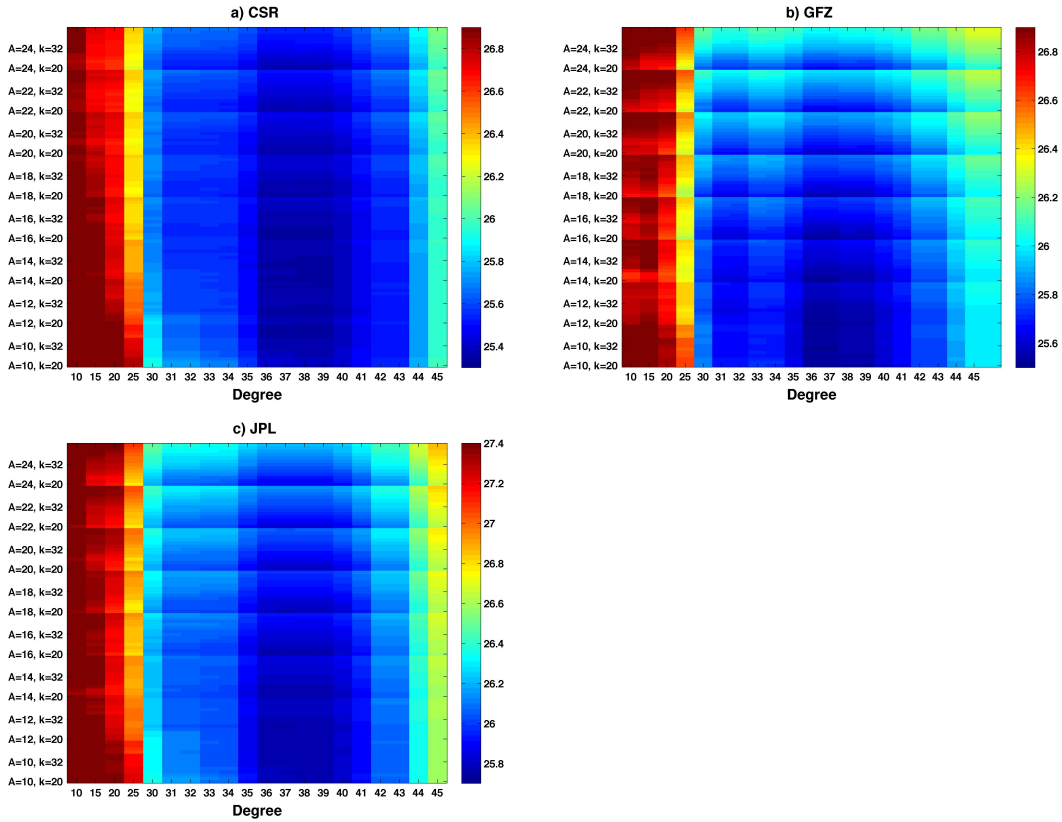


Figure 5. RMS of the differences between synthetic and GRACE data: a) CSR; b) GFZ, and c) JPL. Decorrelation and Gauss ( $r=500$  km) filter applied to GRACE data. Synthetic data truncated at degree 60. Continental leakage reduced. Units: mm.

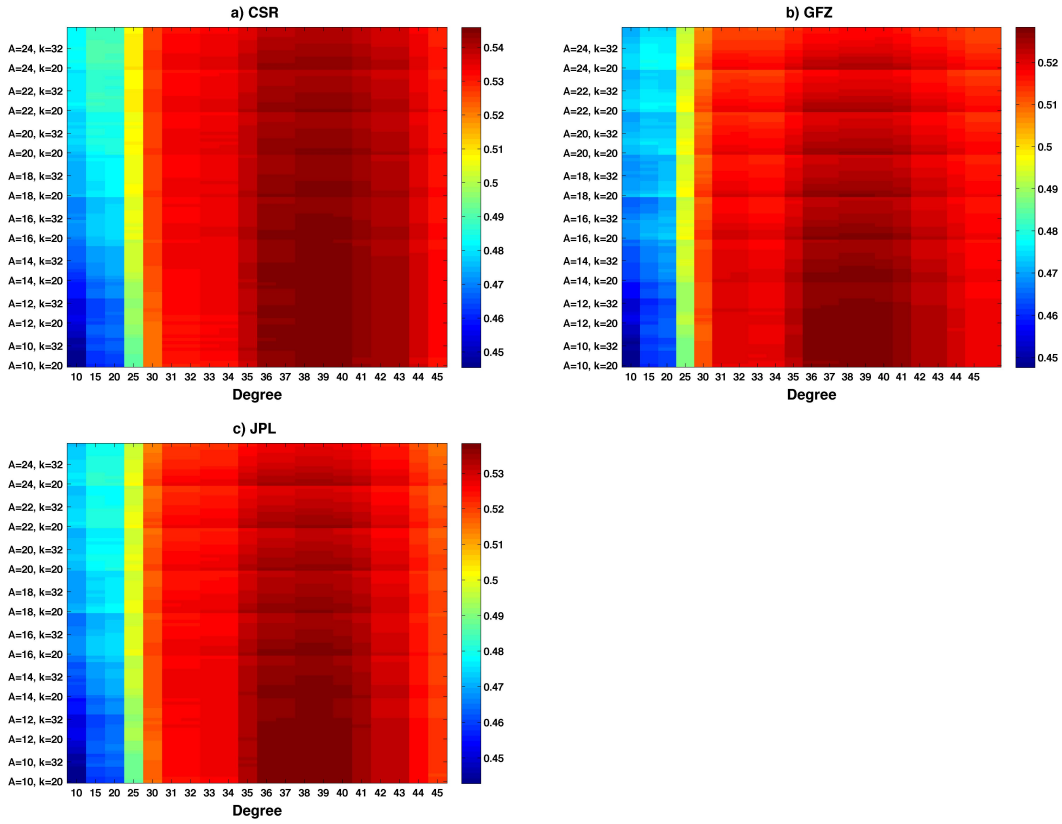


Figure 6. Correlation coefficients between synthetic and GRACE data: a) CSR; b) GFZ, and c) JPL. Data processing as in Figure 5.



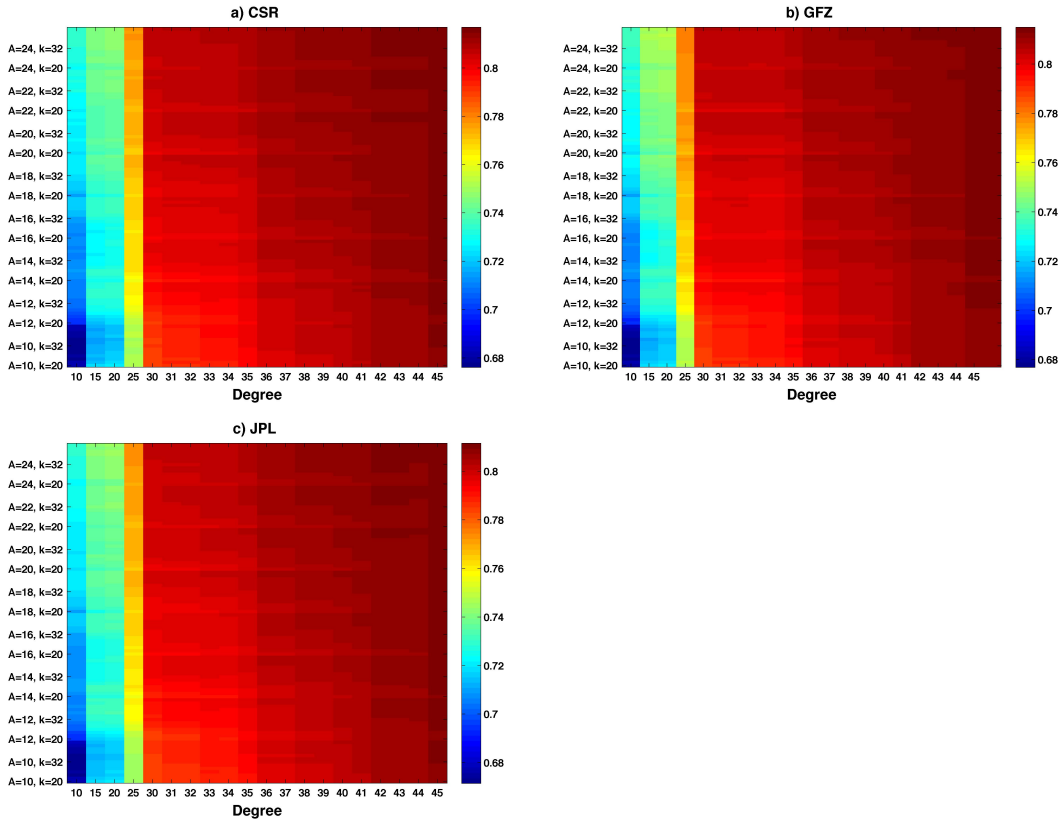


Figure 7. Correlation coefficients between the annual amplitudes of synthetic and GRACE data: a) CSR; b) GFZ, and c) JPL. Data processing as in Figure 5.

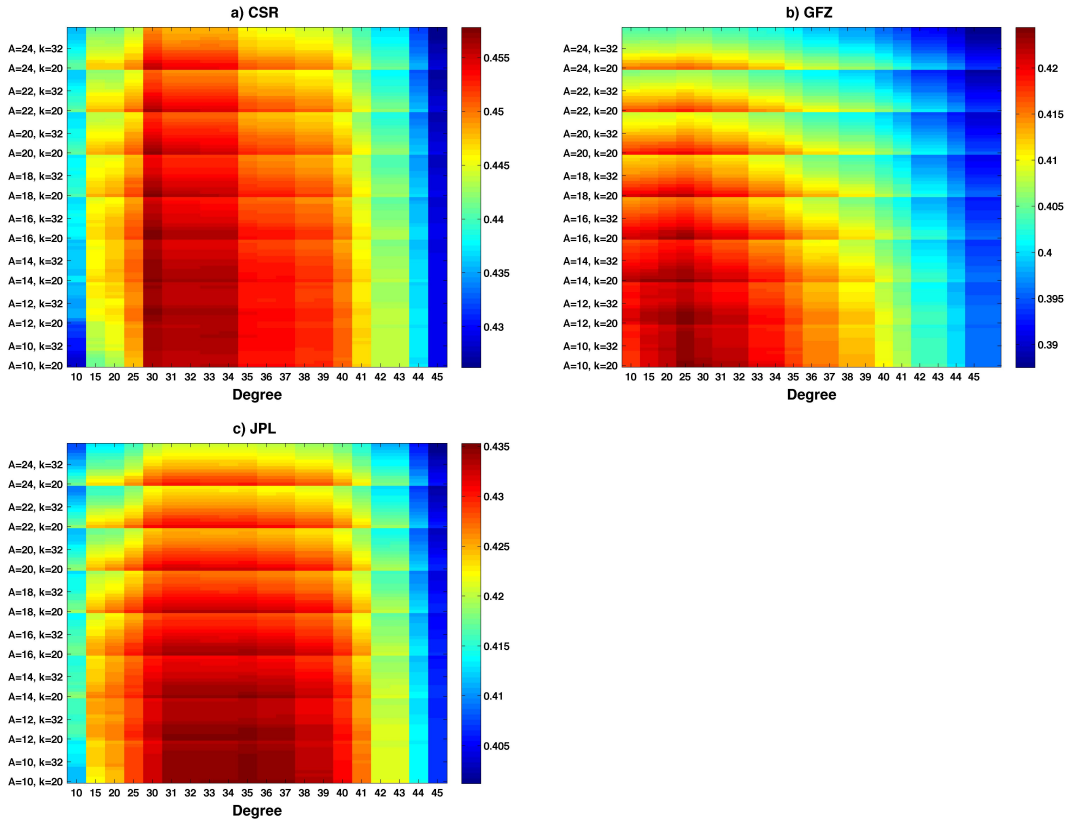


Figure 8. Correlation coefficients between the non-seasonal signals from synthetic and GRACE data: a) CSR; b) GFZ, and c) JPL. Data processing as in Figure 5.

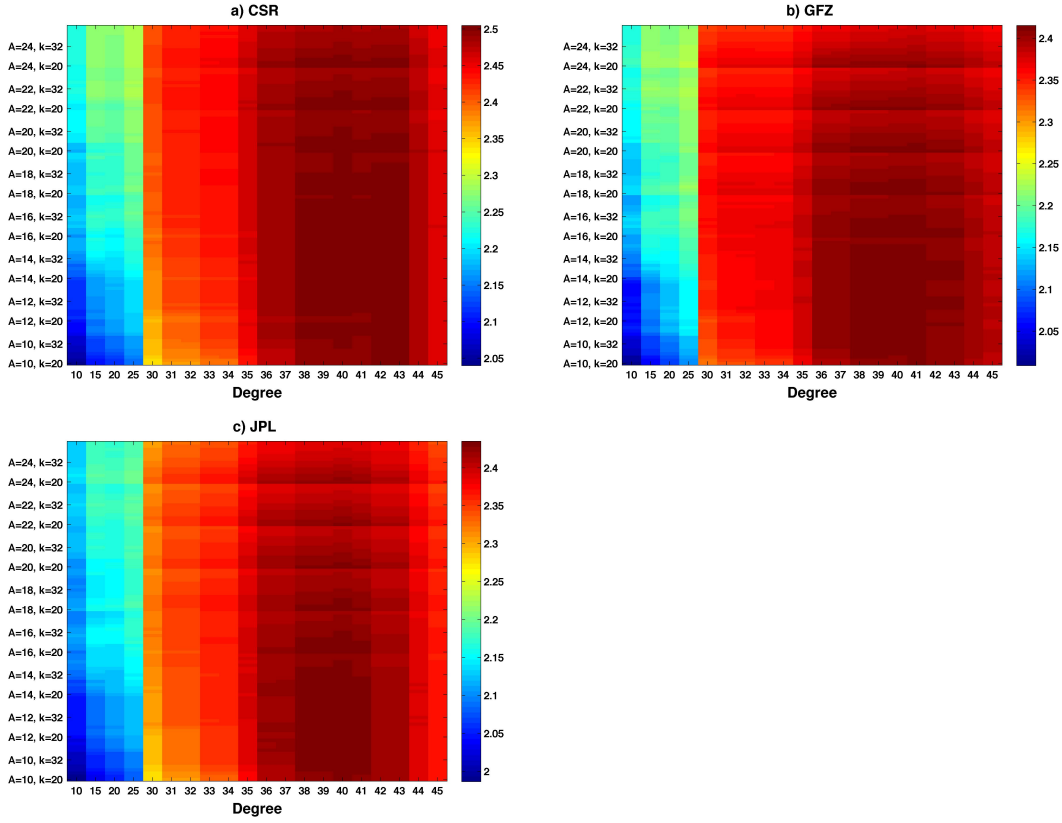
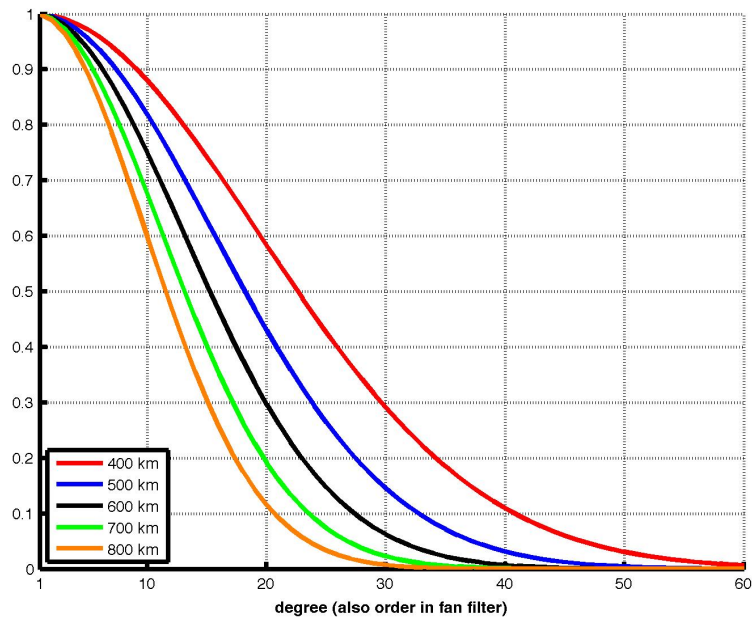
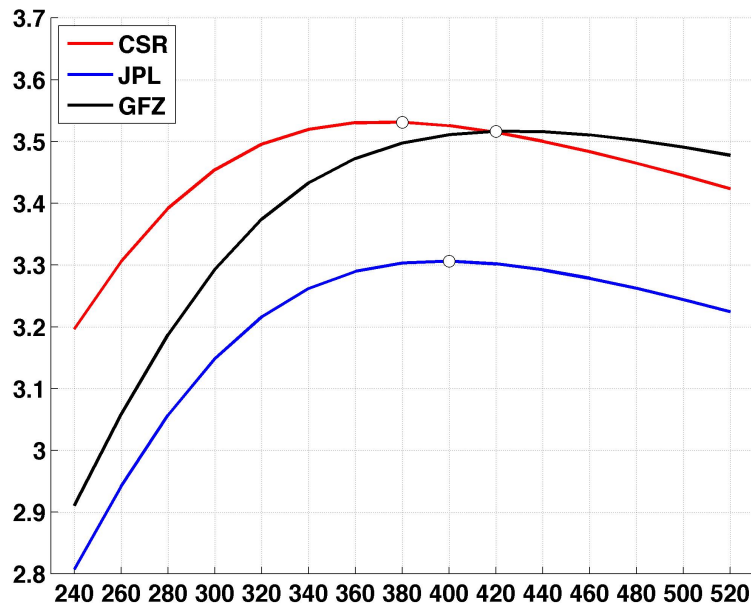


Figure 9: Ratio of variability between the continents and the ocean: a) CSR; b) GFZ, and c) JPL. Decorrelation and Gauss ( $r=500$  km) filter applied to GRACE data. Ocean points closer to 500 km to the continents are avoided.



**Figure 10.** Weights of the Gaussian filter for different radius:  $r=400$  km (red line),  $r=500$  km (blue line),  $r=600$  km (black line),  $r=700$  km (green line), and  $r=800$  km (orange line).



**Figure 11.** Ratio of variability between continents and ocean for GRACE data from: a) CSR; b) JPL; and c) GFZ, as a function of the radius  $r$  of the Gaussian filter. GRACE data have been previously decorrelated. Ocean points closer to 500 km to the continents are avoided.

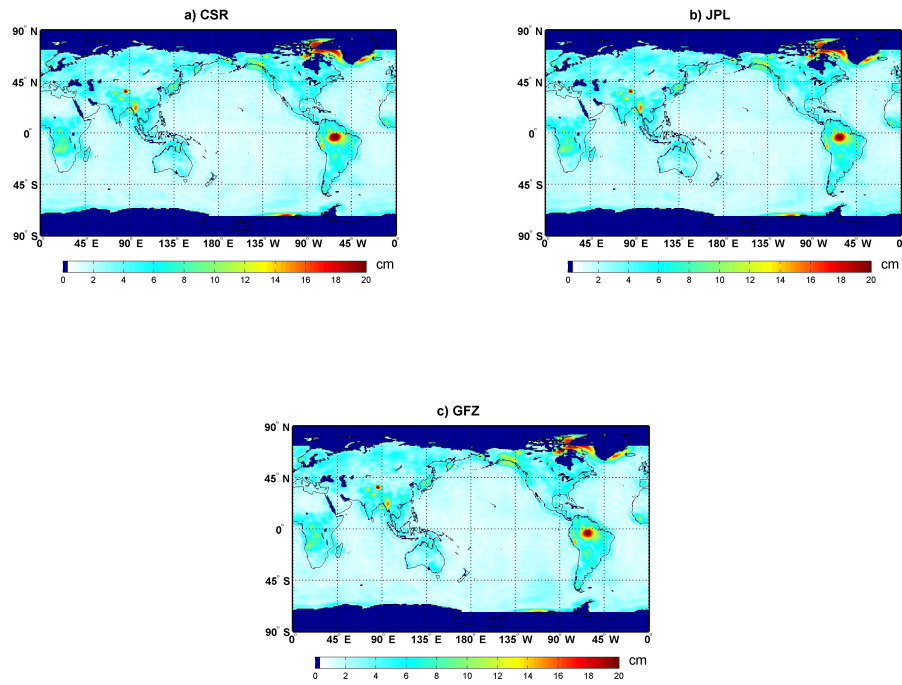


**Figure 12.** Standard deviation of the residual between synthetic and filtered GRACE data: a) CSR; b) JPL; and c) GFZ. Decorrelation and Gauss ( $r=380$  km for CSR;  $r=420$  km for GFZ; and  $r=400$  km for JPL) filter applied to GRACE data. Synthetic data truncated at degree 60. Continental leakage reduced.

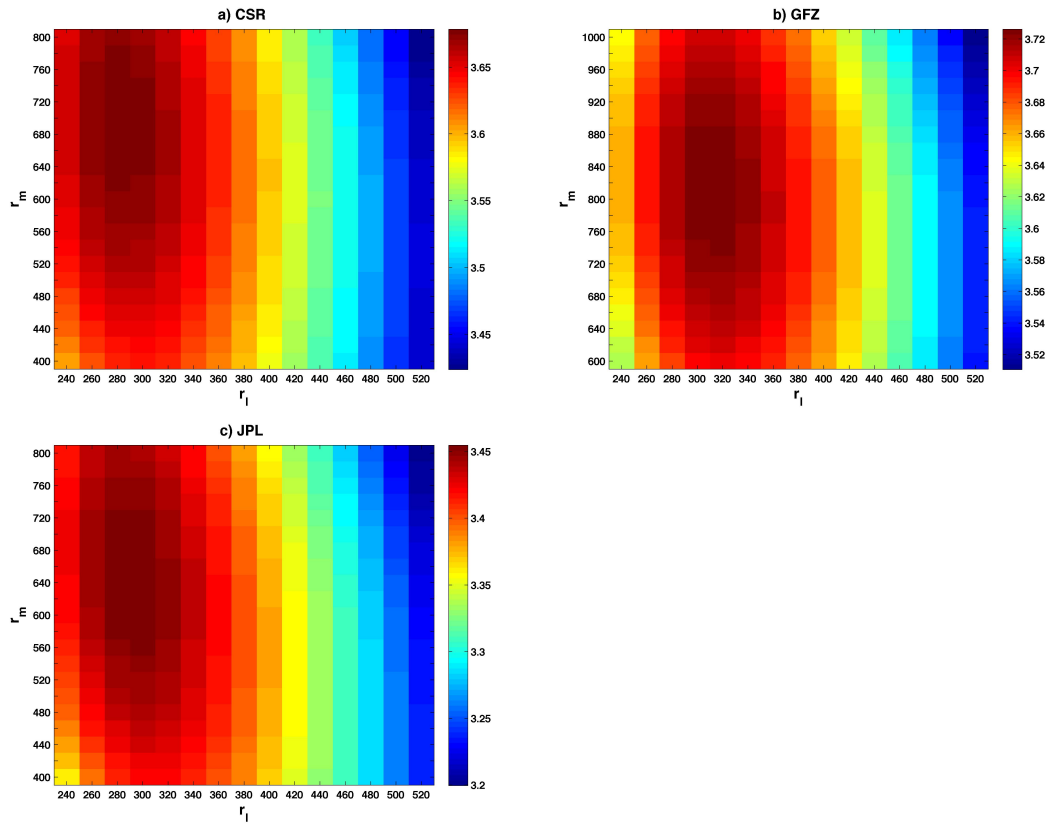


**Figure 13.** Ratio of variability between continents and ocean for GRACE: a) CSR; b) JPL; and c) GFZ, as a function of the radii  $r_l$  and  $r_m$  of the fan filter. GRACE data have been previously decorrelated. Ocean points closer to 500 km to the continents are avoided.